JOURNAL OF MATERIALS SCIENCE: MATERIALS IN MEDICINE 6 (1995) 327–334

Structural characterization of plasma-sprayed hydroxylapatite coatings

R. McPHERSON†, N. GANE
CSIRO Division of Manufacturing Technology, Preston 3072, Victoria, Australia
T. J. BASTOW
CSIRO Division of Materials Science and Technology, Clayton 3168, Victoria, Australia

Plasma-sprayed hydroxylapatite coatings, widely used on metallic surgical implants to improve their adhesion to bone, are formed by rapid quenching of molten, or partly molten, particles which impact the substrate at high velocity. The performance of these coatings in the body depends upon their structure, which is not well understood. Coatings prepared under a range of spraying conditions have been studied by X-ray diffraction (XRD), differential thermal analysis (DTA), thermogravimetric analysis (TGA) and solid-state nuclear magnetic resonance spectroscopy (NMR). The results suggest that particles partly melt and lose combined water at lower plasma torch input powers forming a glass, by quenching of the liquid phase, and an OH-depleted hydroxylapatite residual crystalline phase. At higher power inputs an increasing amount of P_2O_5 is also lost and the coatings contain CaO and $Ca_4P_2O_9$. Heat treatment of coatings in air at 600 °C results in crystallization of the glass phase and reaction with water vapour to form hydroxylapatite. The results show that XRD is relatively insensitive to some of the structural details of hydroxylapatite coatings which may be significant to their performance. NMR provides more structural information and is a significant tool for coating characterization.

1. Introduction

Several companies produce surgical and dental metallic implants with plasma-sprayed hydroxylapatite (HA) coating to promote bone growth and improve the bond between the implant and bone, but details of the procedures used for their manufacture and the coating structures obtained tend to be covered by commercial secrecy. Although plasma-sprayed HA coatings have been used for some time, their structures have not been well defined and reservations remain concerning their effectiveness [1]. An area of particular interest is the solubility of coatings in the bodily environment, which is apparently related to the coating structure [2–5].

Plasma sprayed ceramic coatings are formed from a stream of molten particles produced by injecting a powder, usually with a particle size in the range of 20–50 μm, into a high velocity, high temperature plasma jet where they are rapidly accelerated and melted. The coating is formed by successive impact on the substrate of molten particles each of which spreads to form a disc-shaped lamella a few micrometres thick and solidifies at a cooling rate $> 100\ K\ s^{-1}$. Under these conditions the equilibrium phase may not be retained and metastable crystalline or non-crystalline products may be formed [6]. Under ideal conditions all of the particles are completely melted and a dense coating is produced. In practice, some partly melted particles are also incorporated into the coating; unmelted particles rebound from the coating as it is deposited reducing the deposition efficiency.

The structures of plasma-sprayed coatings are a complex function of many processing variables and a large number of experiments is required for a complete analysis. However, the major factor influencing the extent of melting and chemical decomposition of plasma-sprayed materials of given particle size is likely to be the intensity of the temperature–time excursion experienced by the particles during their passage through the plasma jet which, in turn, is influenced most strongly by the electrical power input to the torch.

A number of studies of plasma-sprayed HA coatings have shown that major structural changes are produced by the spraying process. Wolke *et al.* [7] observed that coatings formed by plasma-spraying in air using a 45 μm powder gave a X-ray diffraction (XRD) pattern consistent with a mostly amorphous coating. However, the hydroxylapatite XRD pattern was recovered after heat treatment in air at 600 °C for 1 h.

†Sadly Professor McPherson died after completing this paper. He made a distinctive contribution to the fields of ceramics and thermal spraying and will be missed by the international community.

0957–4530

Coatings sprayed under similar conditions but using 125 μm powder consisted of a mixture of HA and an amorphous phase. This, together with other published information, implies that coatings containing a substantial proportion of HA can only be prepared using larger particle size powder (> 100 μm) than that generally employed in the plasma-spraying process. Frayssinet *et al.* [3] reported that the amorphous phase content of plasma-sprayed hydroxylapatite coatings, used by them to study *in vitro* solubility, varied from 22 to 62% depending upon spraying conditions. HA has the chemical composition $Ca_{10}(PO_4)_6(OH)_2$ with a Ca/P ratio of 1.67. This ratio may change during plasma spraying. A TEM study of the structure of plasma-sprayed HA coatings on titanium showed that they consisted of a mixture of amorphous material and hydroxylapatite and suggested that, although Ca/P was ~ 1.5 for the crystalline phase, it was ~ 0.8 for the amorphous phase [8]. Raman microprobe analysis of commercial plasma-sprayed HA coatings on Ti from three sources also showed that they contained a considerable proportion of amorphous material [9]. A study of plasma-sprayed HA coatings by XRD and infrared spectroscopy showed that the HA phase observed by XRD was in fact OH deficient and consistent with an oxy-hydroxylapatite (OHA) solid solution [4]. Decomposition of HA during spraying to form CaO and $Ca_3P_2O_8$ has also been reported under certain conditions [10].

The present paper reports an initial study of the influence of torch power on the structural changes which occur during the spraying of a commercial HA powder supplied for the preparation of plasma-sprayed coatings. X-ray diffraction (XRD), nuclear magnetic resonance spectroscopy (NMR), differential thermal analysis (DTA), thermogravimetric analysis (TGA) and microscopic examination were used to characterize coatings prepared over a wide range of torch powers with all other processing parameters held constant. XRD alone is not adequate to resolve the detailed structure of the mainly disordered phases present in HA coatings; NMR spectra were used to provide complementary structural information since they are sensitive to the short range interactions in the solid. To eliminate the effects of dipolar interactions and chemical shift anisotropy, which serve to broaden NMR signals in the solid state, the technique of magic angle spinning (MAS) was used in which the specimen was rotated, at frequencies of order 10 kHz, around an axis at an angle of $\cos\theta = 3^{-1/2}$ ($= 54.7°$) to the magnetic field. The residual linewidths observed in disordered materials (such as the plasma-sprayed HA) arises from chemical shift dispersion, due to the range of environments at the atomic sites, and cannot be removed by sample spinning.

2. Experimental methods

Coatings were prepared using Amdry 6021 HA powder with a mean particle size of 110 μm. The coatings were sprayed using a CSIRO Electronic Plasma Torch [11] on to 25 mm diameter, 6 mm thick disc substrates arranged in a circle 250 mm diameter on supporting arms which were rotated at 72 rpm in front of the torch. Specimens were cooled by an air jet impinging on to the sprayed surface. The torch was oscillated along a diameter of the supporting arms over a distance of 75 mm at a rate of 16 strokes per minute. Powder was injected into the final anode region of the torch through a 1.9 mm diameter port. A range of torch electrical power inputs was employed (10, 15, 22.5, 35, 45 kW) with other plasma-spraying conditions, as shown below, held constant:

Plasma gas (argon) flow rate	$40\,l\,min^{-1}$
Carrier gas (argon) flow rate	$4\,l\,min^{-1}$
Powder feed rate	$32\,g\,min^{-1}$
Torch-substrate distance	75 mm

The stainless steel disc substrates were prepared with an as-ground finish to enable the coatings to be easily stripped for subsequent characterization. Some substrates were grit blasted with 60 mesh alumina to obtain better coating adhesion. These specimens were sectioned, polished and etched for microscopic examination.

A sample of "in flight" sprayed powder was taken by spraying into water at a spray distance of ~ 0.5 m and a power level of 22.5 kW. Samples of this powder and the original powder were examined using scanning electron microscopy.

XRD examination of the coatings was carried out using CuK_α radiation. The proportion of HA present in coatings as an amorphous phase was estimated from the ratio of the integrated intensity of the amorphous hump in the XRD pattern to the integrated intensity of all the lines for the crystalline HA phase. The latter was estimated by multiplying the integrated intensity of the most intense HA (2 1 1) line by the ratio of the total intensity of all of the lines in the JCPDS file to the intensity of the (2 1 1) line, namely, 7.27. The proportions of CaO and $Ca_4P_2O_9$ were estimated from the relative intensities of the (0 0 2) HA, (2 0 0) CaO and (0 4 0) $Ca_4P_2O_9$ lines using calibration mixtures of HA and each of these phases.

NMR spectra for ^1H and ^{31}P were obtained with a Bruker MSL 400 spectrometer in a nominal field of 9.4 T. A magic angle spinning (MAS) probe with a 4 mm rotor was used with rotation frequencies of 12 kHz for ^{31}P and 15 kHz for ^1H. $^{31}P/^1H$ cross-polarization (CP) spectra were taken in order to determine the portion of the ^{31}P spectrum coming form phosphorus nuclei associated with hydrogen. Ammonium di-hydrogen phosphate was used to set the Hartmann/Hahn condition. Although the MAS probe had a designed low ^1H background it was still necessary to subtract this background to obtain the ^1H spectra of the plasma-sprayed coatings. Since the spectra are broader than for crystalline HA and the peak of ^1H signal amplitude from these specimens was lower by a factor of the order 32 (2^5) than from HA powder.

The Ca/P ratio was determined by induction coupled plasma (ICP) atomic absorption spectroscopy. Combined differential thermal analysis (DTA)

and thermogravimetric analysis (TGA) was carried out at a heating rate of 10° min^{-1} to 1500 °C.

Samples of tetracalcium phosphate ($Ca_4P_2O_9$) and oxy-hydroxyapatite (a dehydrated form of HA consisting of a solid solution of hydroxylapatite and oxyapatite) were prepared for reference purposes. $Ca_4P_2O_9$ was prepared by heating an equimolar mixture of $Ca_3(PO_4)_2$ and $CaCO_3$ in a platinum crucible in air at 1500 °C for 24 h followed by rapid cooling to ambient temperature to avoid formation of HA by reaction with atmospheric water vapour [12]. OHA was prepared by heating Amdry HA powder at 900 °C in a vacuum of 4×10^{-3} Pa for 48 h. TGA in flowing air gave a weight increase of 1.3% on heating to 1000 °C at 10 K min^{-1}, followed by holding at this temperature for 1 h, which implies an initial composition corresponding to $Ca_{10}(PO_4)_6(OH)_{0.54}O_{0.73}$.

3. Results

XRD showed that the original powder consisted only of HA. Coatings consisted of crystalline HA and an amorphous phase when sprayed at 10 or 15 kW and HA, amorphous phase and a trace of CaO and $Ca_4P_2O_9$ when sprayed at a torch power of 22.5 kW. At 35 and 45 kW, increasing proportions of CaO and $Ca_4P_2O_9$ were observed (Fig. 1). The phase constitution of the coatings, estimated from XRD, is shown in Table I. XRD also showed that heat treatment at 600 °C for 1 h in air resulted in recrystallization of the amorphous phase with a corresponding increase in intensity of the HA diffraction pattern. The deposition rates were not measured but were clearly quite low when sprayed at 10–15 kW, but satisfactory at 22.5 kW and above.

The Ca/P ratio of coatings increased with torch input power as shown in Fig. 2.

NMR of the original powder showed a sharp resonance for ^1H. This peak is considerably reduced in intensity and subsidiary resonances appeared in the spectra of the coatings, Fig. 3. Similar spectra were observed for the reference OHA specimen.

The NMR ^{31}P spectra also showed a single sharp resonance at ~ 2 ppm in the original powder. This was transformed into two broad, overlapping lines (~ 2 ppm and 5 ppm) in the coatings (Fig. 4). The spectrum of the OHA reference showed a strong resonance at ~ 5 ppm together with four overlapping lines centred at ~ 2 ppm. The spectrum of the tetracalcium phosphate reference showed three sharp peaks at 3–4 ppm. The ^1H–^{31}P cross polarization experiments gave a slightly broadened resonance at ~ 2 ppm in the coatings but overlapping ~ 2 and ~ 4.5 ppm lines for the reference OHA (Fig. 5).

The results of the DTA/TGA annealing experiments are shown in Fig. 6. A broad DTA exotherm was observed between 400 and 700 °C (peaking at 606 °C) for a specimen sprayed at 22.5 kW. Simultaneous TGA in flowing air showed an increase in weight of ~ 1.5% during the exotherm.

Sieve analysis of the original powder and the sample sprayed into water showed a decrease in mean particle diameter had occurred in the plasma flame, from

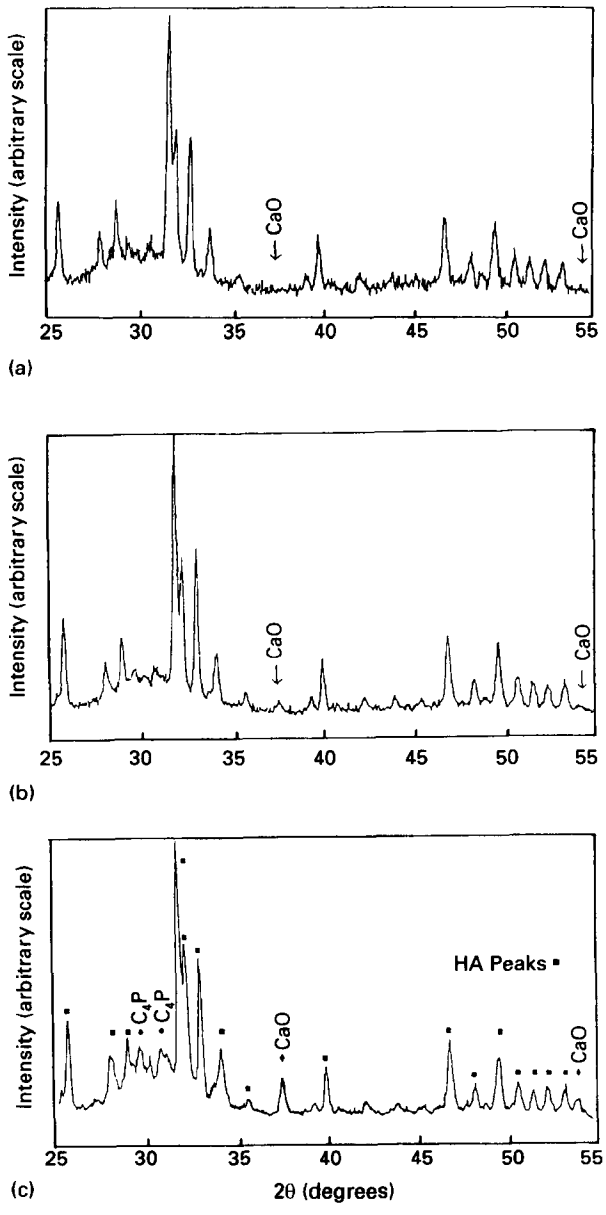

Figure 1 X-ray diffraction patterns (Cu K_α radiation) of HA coatings sprayed at various torch powers: (a) 10 kW; (b) 22.5 kW; (c) 35 kW.

TABLE I Estimated phase constitution of coatings as a function of torch power

Torch power (kW)	% Glass	% HA	% CaO	% $Ca_4P_2O_9$
10	24	76	–	–
22.5	24	66	5	5
35	21	49	10	20
45	18	42	10	20

110 μm to ~ 55 μm, Fig. 7. There was no significant weight difference between powder fed into the flame and powder collected and therefore this decrease could not have arisen through vaporization. Examination of the sprayed powder in the scanning electron microscope showed many small spherical particles that appear to have been fully melted and larger partially melted particles. In many cases partially melted particles showed regions where the underlying

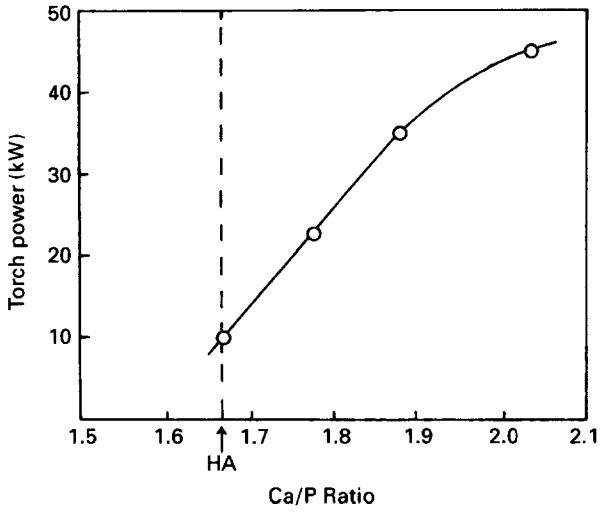

Figure 2 Dependence of Ca/P ratio on torch electrical power input.

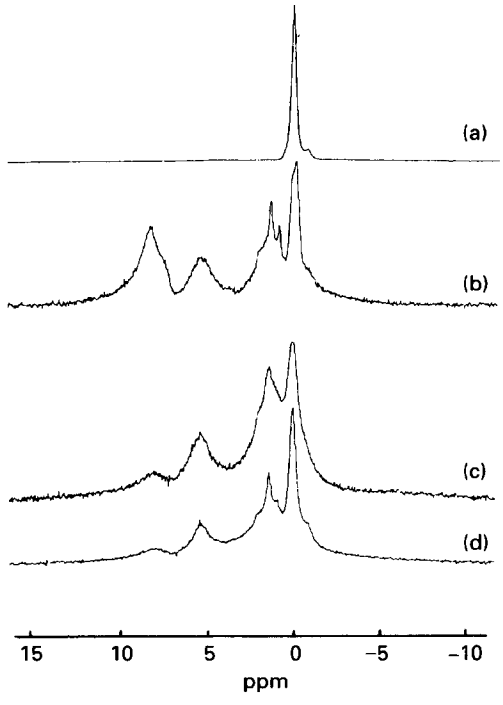

Figure 3 NMR spectra for ^{1}H: (a) HA; (b) OHA; (c) sprayed coating at 10 kW; (d) sprayed coating at 15 kW.

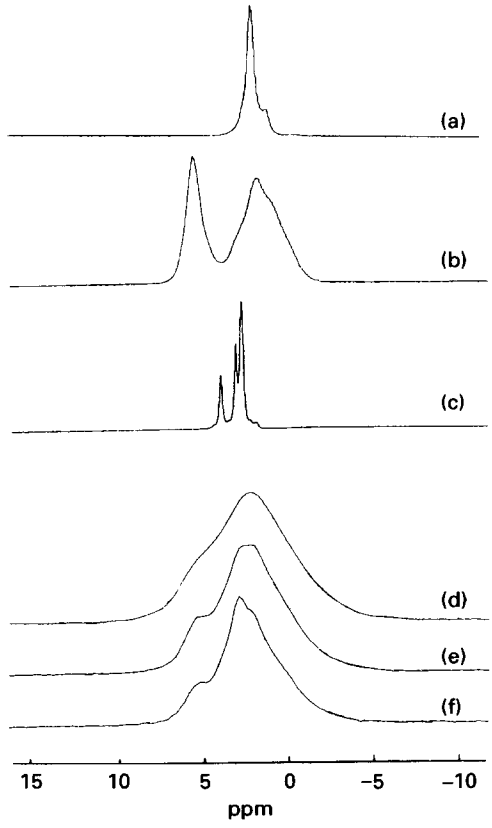

Figure 4 NMR spectra for ^{31}P. (a) HA; (b) OHA; (c) Tetra Ca Phosphate (C_4P); sprayed coatings at (d) 22.5 kW; (e) 35 kW; (f) 45 kW.

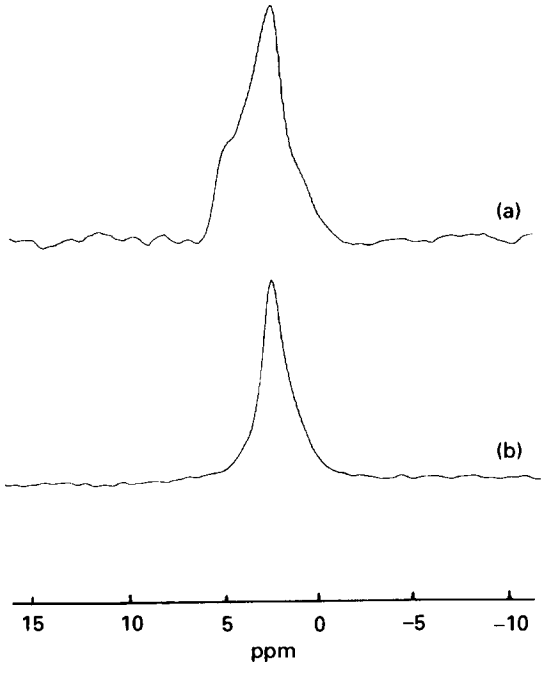

Figure 5 $^{1}H/^{31}P$ cross-polarization spectrum: (a) OHA; (b) sprayed coating at 10 kW.

solid substrate was exposed, Fig. 8. A possible explanation for this eightfold increase in particle number is that the liquid layer forming on the outside of the melting particles is stripped off by the high velocity gas streaming over its surface. The liquid stripped away would subsequently form spherical particles in the gas stream.

Polished and etched transverse sections of HA coatings sprayed at 22.5 kW were examined in the scanning electron microscope. It was found that these coatings etched very rapidly in 0.5% nitric acid to produce strong surface relief, Fig. 9. Many circular and lenticular regions can be seen which remained unetched, surrounded by a strongly etching matrix. The original polishing marks can be seen on the surface of the approximately spherical particle, ~ 20 μm diameter, in the centre of Fig. 9b. The circular form of this particle and the many others present suggests that they might be the remains of much larger solid particles that were fed into the plasma flame. Polished sections of coatings that had been annealed at 600 °C showed quite different structure and etching behaviour with the formation of only light surface relief.

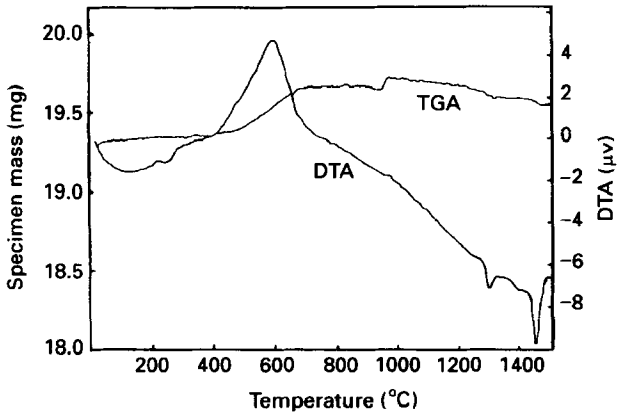

Figure 6 DTA and TGA traces for specimens sprayed at 22.5 kW (heated at 10 K/min in air).

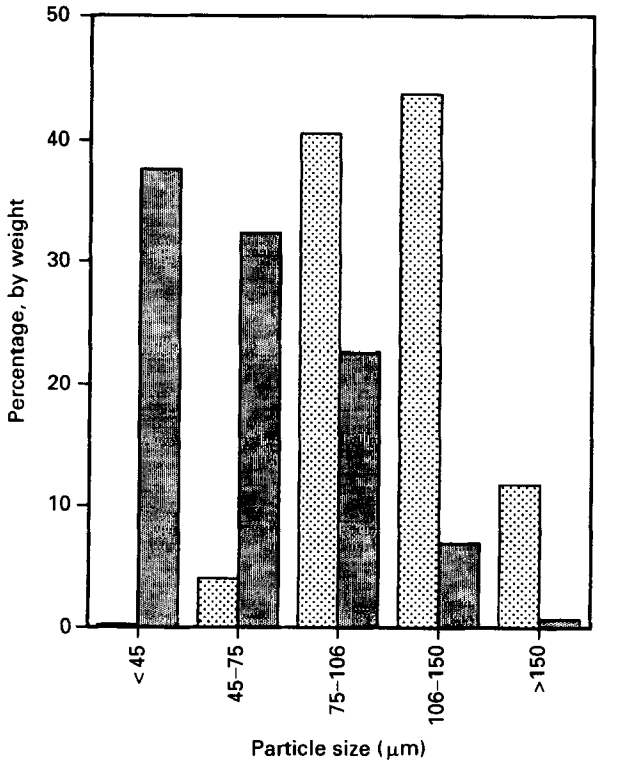

Figure 7 Particle size distribution of as received (▨) and as sprayed (■) HA powder.

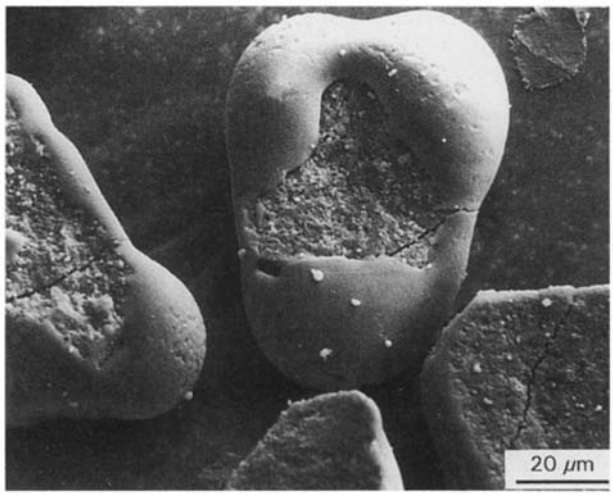

Figure 8 Partially melted HA powder particles collected by spraying into water.

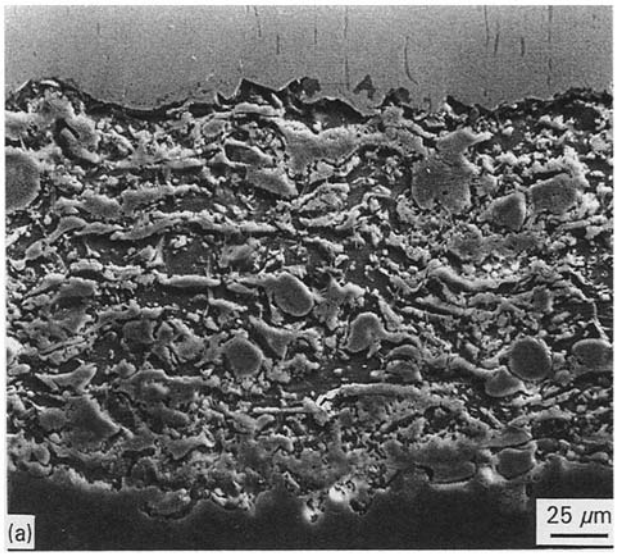

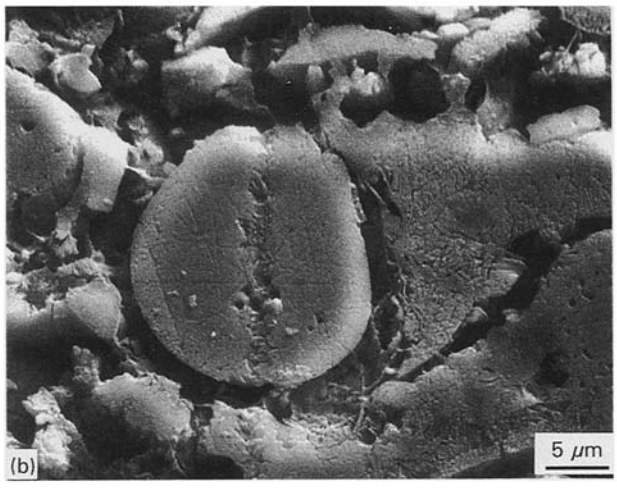

Figure 9 Scanning electron micrographs of an etched cross-section of a sprayed coating (etched 7 s in 0.5% HNO_3).

4. Discussion

Any consideration of the microstructure of plasma-sprayed materials requires background knowledge of the appropriate phase equilibria. The equilibrium phase diagram for the system $CaO–P_2O_5–H_2O$ shows that hydroxylapatite ($Ca_{10}(PO_4)_6(OH)_2$) undergoes incongruent melting, and decomposes at high temperature (T_1) to a mixture of $Ca_3(PO_4)_2$, $Ca_4P_2O_9$ and water, Fig. 10. T_1 depends upon the partial pressure of H_2O increasing from $\sim 1325\,^{\circ}C$ to $\sim 1550\,^{\circ}C$ as the water partial pressure is increased from 6.7×10^2 to 1.33×10^4 Pa; the melting point of the mixture of $Ca_3(PO_4)_2$ and $Ca_4P_2O_9$ formed by decomposition of HA is $\sim 1570\,^{\circ}C$ [13].

It has been shown that the HA crystal structure may be retained if water is partly removed to form a solid solution of hydroxylapatite and oxy-apatite ($Ca_{10}(PO_4)_6O$), the range of composition in "equilibrium" studies [14] being given by:

$$Ca_{10}(PO_4)_6(OH)_{2-2x}O_x\,\square_x \quad \text{where } x \geq 0.75,$$

$\square$ = vacancy

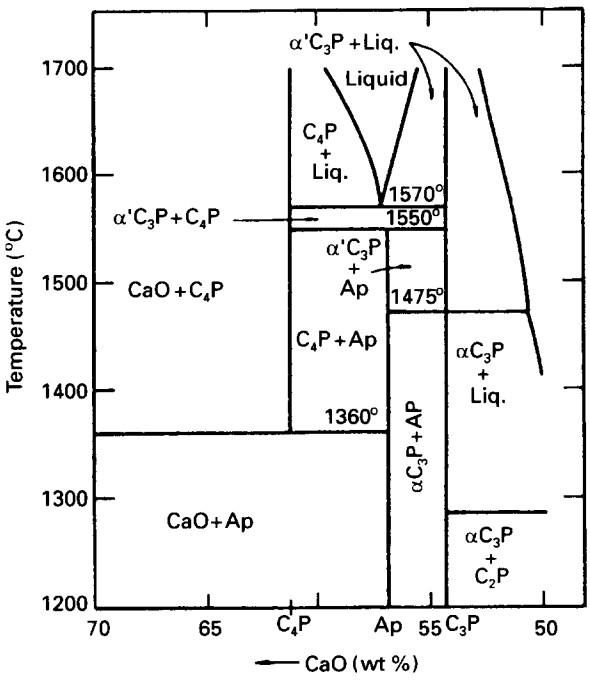

Figure 10 $CaO–P_2O_5$ phase equilibria under a partial pressure of water of $p(H_2O) = 500$ mm (after Riboud [13]).

that is, 75% of the water may be lost whilst retaining the HA crystal structure. The differences in lattice parameter between hydroxylapatite and oxyapatite are reported to be small [15] so that structural changes arising from loss of water are not obvious from XRD patterns. OH depleted HA has been shown to be very reactive, absorbing H_2O at $\sim 600\,°C$ even in a vacuum of 1.33×10^{-2} Pa [14].

Decomposition of HA takes place slowly at temperatures around 1300 °C [13] so that there is the possibility that it melts in a metastable manner without water loss during plasma spraying where the time required to heat to the vicinity of the melting point is only milliseconds. However, increasing loss of H_2O and P_2O_5 from the molten droplets might be expected as the temperature–time regime is increased.

The present XRD results and microscopic evidence suggest that a large proportion of the particles do not melt completely at lower torch powers and the spray plume consists of these partially melted particles and a large number of small fully melted particles. The liquid phase subsequently solidifies to a glass on impact giving a microstructure consisting of HA crystals dispersed in glass.

The DTA results showed that there is a liberation of heat between 400 and 700 °C which may be ascribed to recrystallization of the glassy phase. The increase in weight of 1.5% observed in the TGA experiments in this temperature range may be interpreted as recovery of water lost during the spraying process. The magnitude of this increase suggests that both the crystalline phase and the glass have become heavily dehydroxylated. Full dehydration corresponds to a weight loss of 1.79% while 0.75 dehydration, the maximum sustainable in OHA solid solution [14], corresponds to 1.34% weight loss.

The increasing proportion of CaO and $Ca_4P_2O_9$ observed with increasing torch power input suggests that P_2O_5 is also lost from the powder during spraying at higher torch power (higher temperature–time input to the particles). This was confirmed by the changes in Ca/P observed as a function of torch power (Fig. 2). The values of Ca/P observed are consistent with the phase constitution inferred from XRD, Table I.

More specific information regarding the structure of the sprayed coatings and the reference materials can be obtained from the NMR spectra because of the much greater sensitivity of this technique to short-range interactions compared to XRD. In particular, the ^1H spectra provide information on the position and environment of the hydroxyl groups and the ^{31}P spectra on the position of the (PO_4) tetrahedra.

The sharp peak observed for ^1H in the original HA powder and, at much smaller intensity in the sprayed coatings (Fig. 3), is consistent with previously reported data and arises from linear chains of structurally equivalent OH parallel to the c-axis of the HA unit cell [16]. Loss of water gives an hydroxylapatite–oxyapatite solid solution in which the chains of OH are replaced by chains of OH, O^{2-} and vacancies. Comparison of the coating spectra with the reference OHA spectra suggest that the additional peaks observed in the coatings arise from this structural change.

There are four features common to the ^1H spectra of OHA and the plasma-sprayed specimens, namely peaks at approximately 7.5, 4.6, 2.4 and -1 ppm. The peak near -1 ppm is presumably from regions of the specimen closely approximating crystalline HA. It is difficult to assign unambiguously the other peaks, although it is possible that the peak at 4.6 ppm is due to surface absorbed water.

A broad peak was not observed, as to be expected if OH was present in the glass phase; the relatively sharp $^1H/^{31}P$ cross polarization lines for coatings also show that OH is only present in part of the crystalline component of the coatings and not in the glass. The basic similarity of all the ^1H features, taken in conjunction with the similarity of the ^{31}P spectra, as discussed below, suggests that OHA is a good overall model for plasma-sprayed HA.

The ^{31}P spectra of the HA powder show a sharp resonance at $+2$ ppm, Fig. 4. This is consistent with previous data and corresponds to $(PO_4)^{3-}$ in well defined equivalent positions in the HA crystal [17]. The ^{31}P spectrum of tetracalcium phosphate (C_4P) consisted of three sharp lines, one of which was approximately twice the intensity of the other two. Since the crystal structure [18] indicates four inequivalent P sites per unit cell the strongest peak presumably is a superposition of the resonances from two of these sites with accidental equivalent shifts.

The spectra for the coatings, on the other hand, show a broadened line centred on that observed for HA powder plus an additional broad line of lower intensity at ~ 5 ppm. The relative intensities of the two lines also varied with torch power. At high torch power there is a suggestion of splitting of the more intense line. This may arise from a combined

(unresolved) peak due to the presence of disordered C_4P, together with a second component corresponding to disordered HA.

Condensed phosphates are based on PO_4 tetrahedral units in which phosphorous atoms form five bonds to four surrounding oxygen atoms. The oxygen atoms are either bridging, that is, they form linkages between phosphorous atoms, or terminal, that is, they bond to one phosphorous atom only. This leads to four types of PO_4 units in $MO-P_2O_5$ phosphate systems; (i) branching units with three bridging oxygens and electrically neutral, (ii) middle units, with two bridging oxygens and a negative charge, (iii) end units with one bridging oxygen and a charge of -2, and (iv) monomeric units with a charge of -3 [19]. Broadened MAS NMR lines from these distinct units have been clearly resolved in binary phosphate glasses. Charge considerations, however, indicate that only monomeric $(PO_4)^{3-}$ would be expected around the HA composition. The ^{31}P spectrum for the OHA reference shows two major resonances at ~ 5 ppm and ~ 2 ppm, although the latter consists of at least four overlapping lines, indicating two predominant phosphorous environments. Two types of environment for phosphate ions in HA coatings have also been inferred from infrared spectroscopy [4]. An additional peak reported in the Raman spectrum of coatings, but not observed in crystalline HA [9], may also arise from a similar effect.

The structural difference between HA and OHA is that the linear chains of OH^{-1} in HA are replaced by chains of O^{2-}, OH^{-1} and vacancies suggesting that the two lines observed in OHA may be associated with different distortions of $(PO_4)^{3-}$ units depending upon their positions relative to the ions in the central chains. The coatings spectra also show two major resonances at ~ 2 and 5 ppm although they are broader indicating higher structural disorder, partly reflecting the presence of a significant proportion of glass, and the relative intensity of the 5 ppm line is lower than the reference OHA. It must, however, be noted that the OHA phase in the coatings has been formed by rapid quenching from high temperature whereas the reference OHA was prepared by slow cooling from a lower temperature and it may therefore have a more ordered distribution of the cations and vacancies in the central channels of the unit cell.

The structure of HA coatings prepared by plasma spraying will be related to the thermal cycle experienced by the individual particles in the spray stream. The cycles are not identical for all particles at fixed processing conditions (electrical power input, plasma gas type and flow rate, powder injection conditions, torch substrate distance) because of differences in particle diameter and particle trajectory through the plasma jet. The present experiments have shown that with a relatively large starting particle size particle multiplication occurs in the plasma flame apparently by ablation of the liquid layer on the surface of melting particles. This creates a large flux of small fully melted particles.

The final structure of individual particles is determined by rapid quenching on impact. It has been shown that both plasma-sprayed $Ca_3(PO_4)_2$ and $Ca_4P_2O_9$ coatings are completely crystalline [20] but the present and previous studies suggest that plasma-sprayed HA forms a $CaO-P_2O_5$ glass if the particles are completely melted. Most if not all, of the water is lost from completely molten particles so the presence of water in molten particles cannot be the reason for formation of a glass on quenching. The most likely explanation is the well-known tendency to form amorphous phases on rapid solidification of liquids with compositions in the vicinity of a eutectic [21]. The remaining unmelted particles lose some of the combined water in flight and become incorporated into the coating in a solid form retaining a high-temperature OHA structure. The size of these unmelted regions is quite small, 20–30 μm, compared with the initial HA particle size of ~ 110 μm.

XRD revealed the presence of a significant proportion of $Ca_4P_2O_9$ in coatings sprayed at high torch power. Under these higher temperature–time regimes melted regions also lose P_2O_5 and CaO is formed in the droplets, probably at the particle surface. Rapid cooling of the liquid phase results in crystallization of $Ca_4P_2O_9$ from liquid with Ca/P = 2, and glass from liquid with Ca/P between 1.67 and some critical value < 2.

These results support the view that the coatings consist of a mixture of $CaO-P_2O_5$ glass and a crystalline phase based on OHA. Further work is necessary to determine the coating structures in more detail and to determine whether OHA behaves differently to HA in the bodily environment.

5. Conclusions

Relatively large particle size HA powders (~ 100 μm) are partly melted and lose water during plasma spraying at low torch power ($< \sim 20$ kW) giving coatings which consist of a mixture of $CaO-P_2O_5$ glass, formed by quenching of the liquid phase, and OH-deficient OHA from the residual solid phase. Heat treatment in air at 600 °C results in reaction with traces of water vapour, and crystallization of the glass to form HA. At higher torch powers P_2O_5 is also lost and the coatings contain CaO and $Ca_4P_2O_9$. NMR shows promise as a tool to study the structure of plasma-sprayed HA coatings but further work is necessary to elucidate some of the structural details.

Acknowledgements

The authors are indebted to David Hay for the powder X-ray spectra, to Peter Curtis for the chemical analyses and to Stefan Gulizia for assistance with the plasma spraying and powder preparation. The support of Dr R. Sekel is gratefully acknowledged.

References

1. D. ERICKSON, *Scientific American* August (1991) 86.
2. W. J. SHEN, K. C. CHUNG, G. J. WANG and R. E. MCLAUGHLIN, *J. Arthroplasty* 7 (1992) 43.

3. P. FRAYSSINET, F. TOURENNE, N. ROUQUET, G. BONEL and B. GLAMMARA, Proceedings of International Thermal Spray Conference, Orlando, Florida, USA, June 1992 (ASM International, 1992) p. 477.
4. S. R. RADIN and P. DUCHEYNE, *J. Mater. Sci. Mater. Med.* 3 (1992) 33.
5. H. H. HARRIS, Proceedings of Third National Thermal Spray Conference, Long Beach, California, USA, May 1990 (ASM International, 1991) p. 419.
6. R. McPHERSON, *Thin Solid Films* **83** (1981) 297.
7. J. G. C. WOLKE, C. P. A. T. KLEIN and V. DE GROOT, Proceedings of Third National Thermal Spray Conference, Long Beach, California, USA, May 1990 (ASM International, 1991), p. 413.
8. HUAXIA JI, B. PONTON and P. M. MARQUIS, *J. Mater. Sci. Mater. Med.* **3** (1992) 283.
9. M. WEINLAENDER, J. BEUMER III, E. B. KENNEY and P. K. MOY, *ibid.* **3** (1992) 397.
10. K. A. GROSS and C. C. BERNDT, Proceedings of Second Plasma-Technik Symposium, Lucerne, Switzerland, June 1991 (Plasma-Technik AG, Wohlen/Switzerland, 1991) Vol. 3, p. 159.
11. J. D. VOLRATH, A. DOOLETTE and S. RAMAKRISHNAN, Proceedings International Thermal Spray Conference, Orlando, Florida, USA, June 1992 (ASM International, 1992) p. 117.
12. H. MONMA, M. GOTO, H. NAKAJIMA and H. HASHIMOTO, *Gypsum Lime* **202** (1986) 151.
13. P. V. RIBOUD, *Ann. Chim.* **8** (1973) 381.
14. J. C. TROMBE and G. MONTEL. *Comp. Rend. Acad. Sci.: Paris* **273** (1971) 462.
15. J. C. TROMBE and G. MONTEL, *ibid.* **274** (1972) 1169.
16. J. P. YESINOWSKI and H. ECKERT. *J. Amer. Chem. Soc.* **109** (1987) 6274.
17. T. M. DUNCAN and D. C. DOUGLAS, *Chem. Phys.* **87** (1984) 339.
18. B. DICKENS, W. E. BROWN, G. J. KRUGER and J. M. STEWART, *Acta Crystallogr.* **B29** (1973) 2046.
19. M. VILLA and K. R. CARDUNER, *Phys. Chem. Glasses* **28** (1987) 131.
20. C. P. A. T. KLEIN, P. PATKA, H. B. M. VAN DER LUBBE, J. G. C. WOLKE and K. DE GROOT, *J. Biomed. Mater. Res.* **25** (1991) 53.
21. M. H. COHEN and D. TURNBULL, *Nature* 189 (1961) 131.

Received 16 *May*
and accepted 29 *June* 1994